Supplementary Information (SI) for Nanoscale.

Supporting Information: SnSb as a Long Cycle Life Anode Material for Sodium-Ion Batteries Enabled by a High Concentration Electrolyte

S. O'Sullivan,[a] E. Adegoke,[a] K.M. Ryan,[a] H. Geaney,[a] T. Kennedy*[a]

[a] Bernal Institute and Department of Chemical Sciences, University of Limerick, Limerick V94 T9PX Ireland

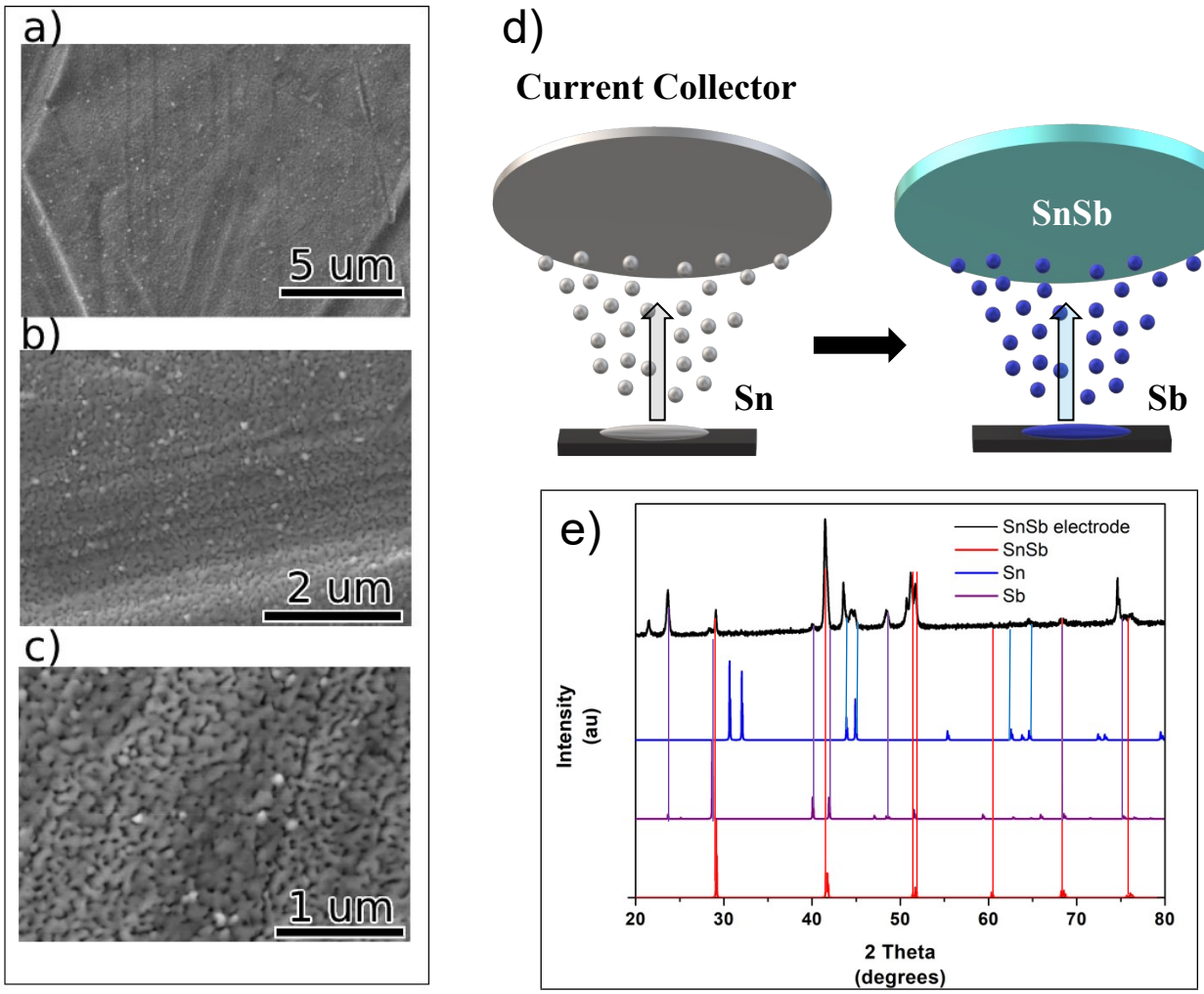

Fig. S1 a, b & c) SEM images of pristine SnSb electrode. d) Diagram of Sn & Sb sequential thermal evaporation onto current collector. e) XRD spectrum of pristine SnSb electrode after preparation by PVD

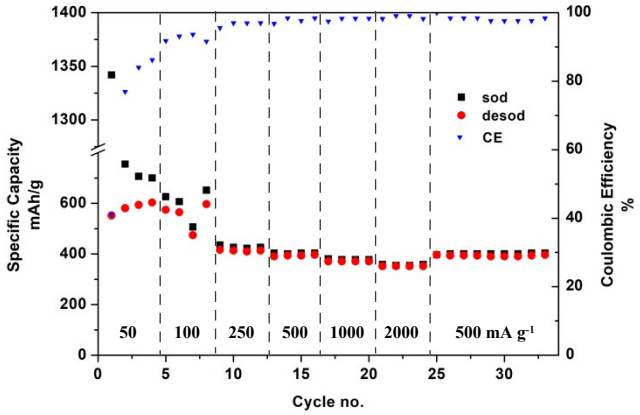

Fig. S2 Charge/discharge rate capability testing and coulombic efficiency for SnSb

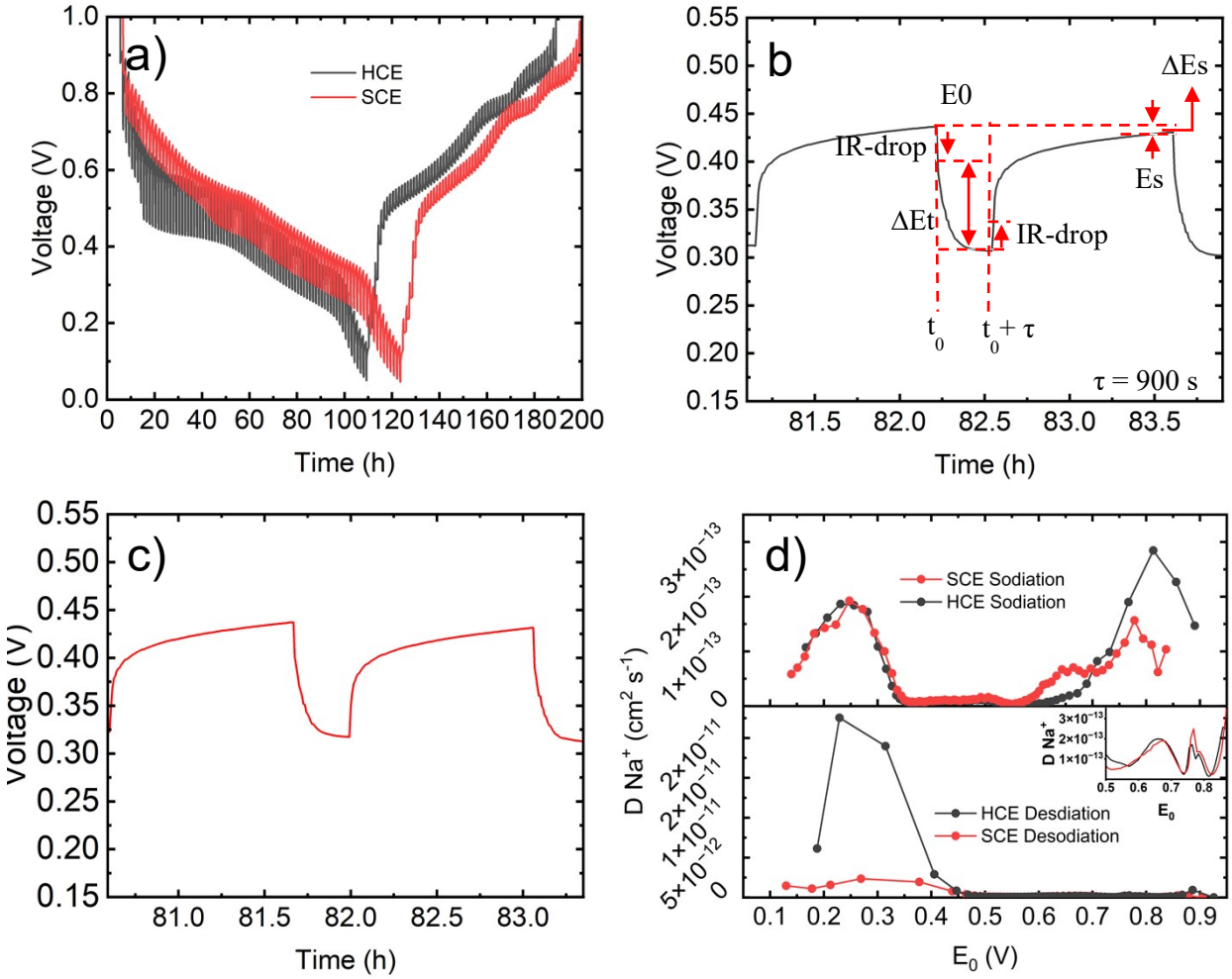

Fig. S3 a) GITT voltage profile recorded for both HCE and SCE, b) typical titre recorded for HCE, and labelling of values used in Na^+ diffusivity calculations, c) typical titre recorded for SCE, d) Na^+ diffusivity as a function of steady state voltage for both sodiation (top) and desodiation (bottom), with inset showing diffusivity during desodiation at a smaller scale.

Galvanostatic intermittent titration technique (GITT) was used to compare the Na^+ diffusivity in SnSb in each electrolyte. Ficks second law can be used to calculate Na^+ diffusivity. This has been adapted for GITT as follows: (1-5)

$$D_{Na^+} = \frac{4}{\pi\tau}\left(\frac{m_B \cdot V_M}{M_B \cdot S}\right)^2\left(\frac{\Delta E_s}{\Delta E_\tau}\right)^2 \qquad \text{eq [1]}$$

Where D_{Na+} is the solid state diffusivity of Na^+, τ is the current pulse duration, m_B is the active mass of the electrode, V_M is molar volume, M_B is molar mass, S is electrochemically active surface area, E_S is quasi-steady state voltage at the end of the relaxation phase, and E_τ is voltage change as a result of the current pulse. With alloying anodes undergoing large volume change during (de)sodiation, finding a value for S that is accurate as a function of voltage is challenging. Similarly molar volume will vary as a function of voltage. For the purpose of comparing the impact of electrolyte concentration on D_{Na+} this was simplified to using geometric area of the electrode for S, (1, 2, 4, 5) however the findings should not be directly compared to similar SnSb electrodes in literature. Constant current pulses with a rate of C/30 were applied over 900 seconds, followed by a 1 h relaxation at open-circuit potential.

GITT was performed for both sodiation and desodiation in the voltage range of 0.05 – 1V. at 25^{O}C. Fig. S3a presents the voltage profiles for both SCE and HCE GITT experiments. Typical examples of titration peaks are shown in Fig. S3b and Fig. S3c for HCE and SCE respectively. Fig S3b also highlights how the values used in calculating Na^+ diffusivity were acquired. Na^+ diffusivity as a function of steady-steady voltage in SnSb in both electrolyte systems is displayed in Fig. S3d.

Diffusivity increased during initial sodiation to a maximum of 3 x 10^{-13} cm^2 S^{-2} at 0.80V for the HCE system, and 1.6 x 10^{-13} cm^2 S^{-2} at 0.78V for the SCE system. D_{Na+} in SnSb in the HCE system remains greater than in SCE above 0.71V, but in SCE the diffusivity is greater from 0.55 V to 0.70 V. From both the differential capacity and voltage profile plots, shown in Fig. 1 b and c respectively, Sb sodiation begins to occur at ~0.75V, meaning that HCE allows greater D_{Na+} initially, with the SCE facilitating greater D_{Na+} as the process continues. Below 0.55 V D_{Na+} is the same in both electrolyte systems. Both show a minimum D_{Na+} in the range of 2 – 6 x 10^{-15} cm^2 S^{-1} from 0.35 - 0.55 V in SCE and 0.35 - 0.60 V in HCE. Below 0.35V both electrolytes show almost identical trends increased diffusivity to 2 x 10^{-13} cm^2 S^{-1} at 0.25 V, before decreasing again.

Diffusivity during desodiation shows a more dramatic difference between the electrolyte systems, with D_{Na+} in SnSb in HCE being significantly higher between 0.18 and 0.45 V at 2.3 x 10^{-11} cm^2 s^{-2}.D_{Na+} in the SCE system also increases in this voltage range but is a magnitude lower at 2.3 x 10^{-12}. This

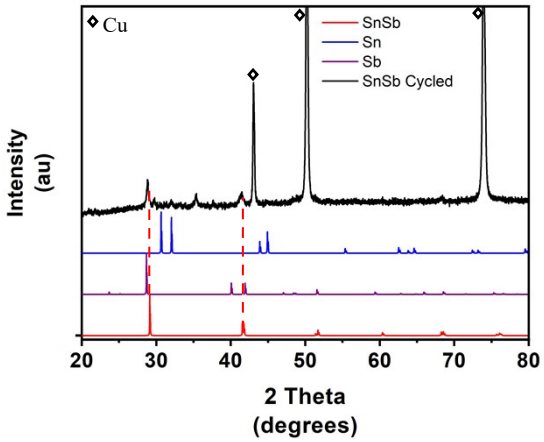

correlates with Na_xSn desodiation (6, 7), demonstrating that HCE better facilitates this process. Both

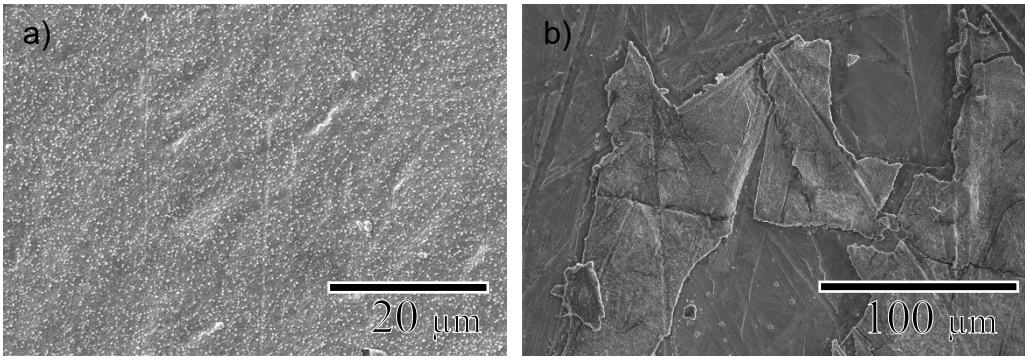

electrolytes show very similar diffusivity throughout the rest of the desodiation with D_{Na+} in the range of 1-2 x 10^{-13} for both electrolyte systems throughout most of the desodiation. Twin peaks at 0.77 and 0.79 V are present in both electrolyte systems, but diffusivity marginally higher in HCE as can be seen in the inset in Fig S3d. This is in the voltage range where Sb desodiation occurs. (7)

Fig. S4 XRD for post-mortem SnSb electrode after 3 cycles

Fig. S5 Increased mass loading SnSb on planar stainless steel. a) Pristine and b) post-mortem

1. Rui X, Yesibolati N, Li S, Yuan C, Chen C. Determination of the chemical diffusion coefficient of Li+ in intercalation-type Li3V2 (PO4) 3 anode material. Solid State Ionics. 2011;187(1):58-63.

2. Gao H, Gao W, Pumera M. 3D‐Printed Nanostructured Copper Substrate Boosts the Sodiated Capability and Stability of Antimony Anode for Sodium‐Ion Batteries. Advanced Functional Materials. 2024;34(19):2310563.

3. Jia JH, Bai J, Yang CC, Jiang Q. Scale Construction of “Breathing” Bi/N-CNSs Quasi-Array Structure with Hierarchical Bi Distribution for Sodium-Ion Battery. Nano Letters. 2024;24(37):11393-402.

4. Marker K, Reeves PJ, Xu C, Griffith KJ, Grey CP. Evolution of structure and lithium dynamics in LiNi0. 8Mn0. 1Co0. 1O2 (NMC811) cathodes during electrochemical cycling. Chemistry of Materials. 2019;31(7):2545-54.

5. Wen B, Sayed FN, Dose WM, Morzy JK, Son Y, Nagendran S, et al. Surface reduction in lithium-and manganese-rich layered cathodes for lithium ion batteries drives voltage decay. Journal of Materials Chemistry A. 2022;10(41):21941-54.

6. Li T, Gulzar U, Bai X, Lenocini M, Prato M, Aifantis KE, et al. Insight on the failure mechanism of Sn electrodes for sodium-ion batteries: Evidence of pore formation during sodiation and crack formation during desodiation. ACS Applied Energy Materials. 2019;2(1):860-6.
7. Fehse M, Sougrati MT, Darwiche A, Gabaudan V, La Fontaine C, Monconduit L, et al. Elucidating the origin of superior electrochemical cycling performance: new insights on sodiation–desodiation mechanism of SnSb from operando spectroscopy. Journal of Materials Chemistry A. 2018;6(18):8724-34.